https://doi.org/10.48048/tis.2023.5038

Experimental and Numerical Analysis of the Performance of Various Damper Materials

Mithun Premnath* **and Kriparaj Kareveliparambil Gopi**

Kunjali Marakkar School of Marine Engineering, Cochin University of Science and Technology, Kochi 682022, Kerala, India

(*Corresponding author's e-mail: mithun.premnath@gmail.com)

Received: 1 July 2022, Revised: 25 August 2022, Accepted: 1 September 2022, Published: 5 April 2023

Abstract

The vibration in ships causes structural fatigue, damage to electrical and mechanical devices, excessive level of noise and discomfort to the passengers and crews. Sometimes the increase in ship vibration leads to unsafe operating conditions and thereby discarding it. Thus, the research on vibration reduction is essential in the maritime field and this paper deals with the reduction of vibrations in marine machinery using elastomeric bearings. The numerical analysis of the performance of passive vibration isolators with different damping materials was conducted using ANSYS and the results are validated experimentally. With the help of a vibration exciter, vibration transmissibility at different frequencies is plotted and the hysteresis curve was generated numerically by applying a cyclic load to the bearing. Then, the best damping material was deducted by comparing the calculated loss factor of different elastomeric materials such as natural rubber, styrene-butadiene rubber and polybutadiene Rubber (PBR) and their combinations. The natural rubber blended with styrene-butadiene rubber (SBR) and polybutadiene rubber (PBR) shows an increase in the damping property of the elastomer and can be used for high-frequency damping applications.

Keywords: Damping material, Hysteresis, Elastomers, Loss factor, Vibration

Introduction

The machine vibrations are dangerous as they increase the rate of wear and tear on machine components, which leads to frequent downtime of machinery, loss of production, increased cost of maintenance etc. The vibrations in ship hulls and machinery lead to a reduction in the life of the system and significantly affect the safety of crews and passengers. Since vibrations are unavoidable for a dynamic system, an effective method to eliminate undesirable vibrations should be implemented. Over the years, a lot of active and passive control techniques were employed to reduce the vibration of machinery. Passive vibration control techniques gain priority over active techniques due to their simplicity, ease of implementation, reduced cost and energy consumption. However, there is space for research and development in the field of vibration reduction using passive vibration isolators.

Krishnamoorthi *et al.* [1] noted that natural rubber mounts are vulnerable to oil and damage at high vibrations, and developed new fluorocarbon mounts to avoid the drawbacks of natural rubber mounts. After evaluating the transmissibility, it was concluded that fluorocarbon mounts performed better than rubber mounts. Wan *et al.* [2] carried out a vibration and damping analysis of a multi-layered composite plate with a viscoelastic mid-layer. It was found that multi-layered plates are effective in reducing the natural frequency of the isolators and able to achieve a higher structural loss factor. Moreover, the loss factor does not depend on thickness but depends on the material combination for different layers.

The significant characteristics of nonlinear isolators such as shifts in resonance frequency, jump phenomena, chaotic motion, and internal resonance are used to study the advancements in metallic and viscoelastic nonlinear vibration isolators by Ibrahim [3]. Chavan *et al.* [4] did a comparative study on anti-vibration mounts for vibration isolation in diesel engine generators set with natural rubber and neoprene. For effective isolation, transmissibility should be less than 0.4 and the numerical results showed that neoprene material gave higher vibration isolation than natural rubber. Valeev *et al.* [5] conducted a study on quasi-zero stiffness isolators, which can isolate vibration with very low stiffness. This means that the stiffness of the isolators is close to zero and helps to isolate vibrations with low frequency. Moreover, it was noted that quasi-zero stiffness can be achieved by proper geometric modelling of the isolator and the natural frequency of the developed isolator is found to be less than 1 Hz.

Bharat *et al.* [6] numerically analysed an anti-vibration mount for a traction machine assembly of an elevator. It was concluded that the natural frequency of the anti-vibration mount is 288.62 Hz which is certainly the safe frequency where no resonance can occur for the particular structure. Also, the analysed structure can bear the applied cyclic load which states the structure is analytically safe. Devi *et al.* [7] conducted an experimental study of the elastomeric bearings used in bridges and the elastomeric bearings were designed according to Indian Roads Congress (IRC) 83 standards. The unreinforced elastomeric bearings can return to their original shape on removal of the load and the elongation can range up to more than 10 times their original dimensions. Ahmadipour and Alam [8] conducted a sensitivity analysis of mechanical characteristics of lead core steel-reinforced elastomeric bearings under cyclic loading and noted that the vertical stiffness of elastomeric rubber bearings is dependent on the number of rubber layers. Moreover, the vertical stiffness increases with an increase in the number of layers of the isolator.

Mathai and Manasa [9] found that the damping of lead rubber bearings is very high compared to the damping of laminated rubber bearings. Das *et al.* [10] conducted a study on fibre-reinforced elastomeric base isolators. The study compares the performance of circular and rectangular bearings by the calculation of the effective stiffness of the bearing. It was found that the horizontal stiffness reduces with an increase in maximum displacement. Moreover, the loss factor increase with a reduction in stiffness of the isolator and the loss factor of up to 28 % can be achieved in the case of laminated rubber bearings. Moon *et al.* [11] fabricated a fibre-reinforced elastomeric bearing that shows the same mechanical property as the steel-reinforced bearing. The experimental results were in good agreement with the theoretical results.

Krishnamoorthy and Jayavel [12] conducted static and dynamic analysis in ANSYS for the 3 vibration isolators for heavy load machines. The first model for an existing spring isolator and the other 2 redesigned models are made of helical springs with a parabolic shape part and a spherical ball part. The redesigned models were found to be effective in vibration isolation for heavy loads. Barale and Gawade [13] analysed the different types of passive vibration isolation systems like mechanical springs, spring dampers, elastomeric isolators, tuned mass dampers etc. Lavhande and Tuljapure [14] compared the vibration transmissibility of non-metallic vibration isolators made of cork, rubber and neoprene at different speeds. The Root Mean Square (RMS) value of acceleration was measured with and without isolators at different speeds. Also, the ratio of acceleration with isolators to that without isolators was taken to calculate transmissibility. It was concluded that neoprene is the most effective among the three materials based on vibration transmissibility.

Geethamma *et al.* [15] discussed the key factors that influence vibration damping in polymers like viscoelasticity and glass transition temperature. Moreover, the paper explains different types of damping like Coulomb damping, viscous damping and hysteresis damping. When a solid is deformed, heat is dissipated by internal friction is called hysteretic damping and the area of the resulting hysteresis loop represents the energy loss. Lee *et al.* [16] conducted a study on the possibility of an air-filled rubber membrane for reducing ship propeller-induced vibrations. It was found that the air cavity can help in reducing vibrations. When a pressure wave comes across an air cavity, it gets reflected and at the frequency of destructive interference, the reflected wave will be out of phase with the incident wave due to which they will cancel each other, thereby reducing vibrations and sound. These findings can clarify the working of air cavities that are provided inside the multi-layered vibration isolator.

Moshrefi-Torbati *et al.* [17] investigated a novel design of vibration isolators for space applications. It was a combination of passive and active damping systems to achieve transmissibility of about 19 dB over a range of 1 - 250 Hz. Moreover, the study on the effect of environmental parameters on the performance of damping materials concluded that the properties of the damping materials change in harsh environments. Hence it was proposed to develop the isolator without using viscoelastic elements. Zhao *et al.* [18] prepared a composite material made from natural rubber, nitrile butadiene rubber and hindered phenol. The simultaneous strain-induced orientation and strain-induced crystallisation gave the composites a unique stress-strain behaviour and mechanical characteristics. In the working range of temperatures of seismic isolation bearing where the composites, particularly the Natural rubber/Nitrile butadiene rubber/Hindered phenolic antioxidant (50/50/20) composite, shows high loss factor, high loss peak area, and high hysteresis energy. Emad and Hamid [19] did a numerical study on unbonded fibre-reinforced elastomeric isolators (FREIs) and generated a cyclic load-displacement hysteresis loop. The results of the uniaxial tensile test on the rubber specimen and preliminary cyclic shear tests on a prototype isolator are incorporated to calibrate the model. It serves as a valuable tool to finalize the preliminary design and curb the expensive costs of test repetitions required to achieve the optimized isolator design. Kalfas *et al*. [20] conducted a numerical study on the steel-laminated elastomeric bearing. It was observed that local and global tensile stresses might be developed in bearings under seismic excitations. The analyses showed that steel-laminated elastomeric bearings exhibit local tensile stresses, which alter significantly their stiffness and damping ratio. Wei *et al.*

[21] conducted an experimental and analytical investigation to characterize the influence of compressive load on rate-dependent high damping rubber bearings. The strain rates and compressive stresses applied on specimens were varied and analysed. Finally, comparing the numerical simulations and experimental data obtained from both material tests and full-scale bearing tests, the results were converging and the validity of the proposed model was demonstrated. Significant difference obtained from the experimental results suggested that the influence of compressive load on the instantaneous response of HDR should be taken into account.

A passive vibration isolator uses the inherent properties of the isolation device (i.e., stiffness and damping) to mitigate vibrations and therefore requires no external power source to store or dissipate energy. This paper deals with the reduction of marine machinery vibration using elastomeric bearings along with a comparative study of the performance of the various damper materials. The numerical and experimental analysis of the performance of the vibration isolator made of Natural Rubber (NR), Styrene Butadiene Rubber (SBR), Neoprene (CR), a combination of Natural Rubber and Styrene Butadiene Rubber (NR-SBR), and a combination of Natural Rubber and Poly Butadiene Rubber (NR-PBR) are conducted.

Problem definition and methodology

The main objective of this study is to determine the best passive vibration isolator among Natural Rubber (NR), Neoprene (CR), Styrene Butadiene Rubber (SBR), Poly Butadiene Rubber (PBR) and their combinations based on their damping ability. The combinations of elastomers are made according to parts per hundred rubber ratios. The initial investigation is to determine a better passive vibration isolator among Natural Rubber (NR), Styrene Butadiene Rubber (SBR) and Neoprene (CR). Thereafter the effect of the percentage composition of material on the vibration isolator was evaluated by taking 100 % NR, NR-SBR (25:75), NR-SBR (50:50), NR-SBR (75:25) and 100 % SBR. Then, the effect of the combination of different materials on damping was evaluated by taking NR-SBR (50:50) and NR-PBR (50:50). For comparison, the geometry of all the elastomers was taken as $125 \times 200 \times 20$ mm^3. The loss factor of the elastomeric bearing was calculated by finite element modelling of elastomeric bearings and also validated experimentally by vibration test.

Experimental analysis

Elastomeric bearings with different elastomeric materials such as Natural Rubber (NR), Styrene Butadiene Rubber (SBR), Neoprene (CR), Poly Butadiene Rubber (PBR) and their combinations are fabricated from Middle East Rubber and Engineering, Edayar, Kerala. The elastomeric compounds can be molded or extruded into the required model. The technique is selected based on the part's size, expected quantity, type, and cost of raw materials. Here, the elastomers are fabricated using the molding technique, where the elastomeric material is compressed using a hydraulic press at 22,000 psi pressure.

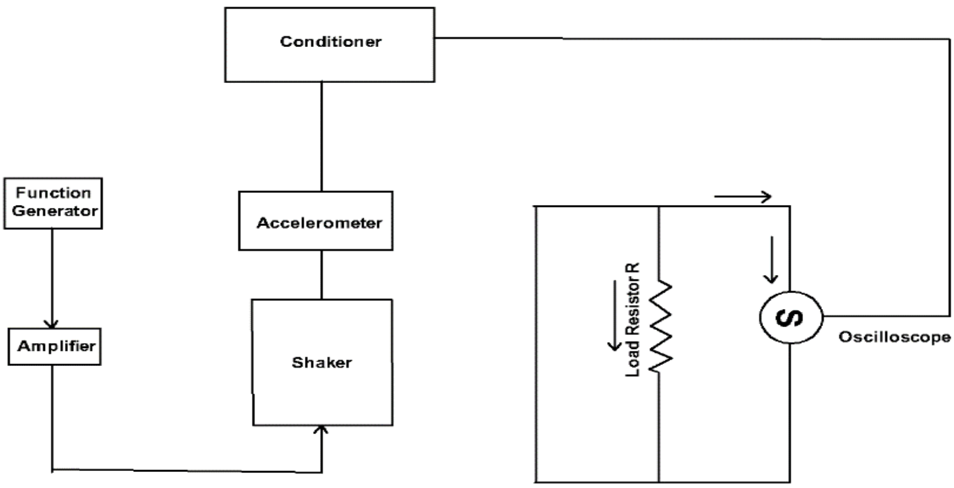

Figure 1 Schematic representation of vibration exciter.

Figure 1 shows the schematic diagram of the vibration exciter. The vibration exciter consists of a shaker table which is actuated using an electric motor and there is a function generator to control the vibration. In a vibration test apparatus, the vibration isolator is mounted on a shaker. The elastomeric bearing is fixed on the shaker using 4 double-sided tapes. The base of the shaker on which the elastomer is mounted is subjected to a harmonic vibration excitation and the transmissibility curves are generated by the controller. The elastomeric bearing's loss factor is determined using the half-power bandwidth (**Figure 2**) or 3 dB approach using transmissibility curves acquired from actual experimental testing. The Loss factor (η_i) for Eigen mode (i) can be calculated from this spectrum using Eq. (1), where f_2 & f_1 are the frequencies at half power points ($0.707\times A_{max}$) and f_0 is the resonance frequency.

$$\text{Loss factor } (\eta_i) = (F_2 - F_1)/ F_0 \tag{1}$$

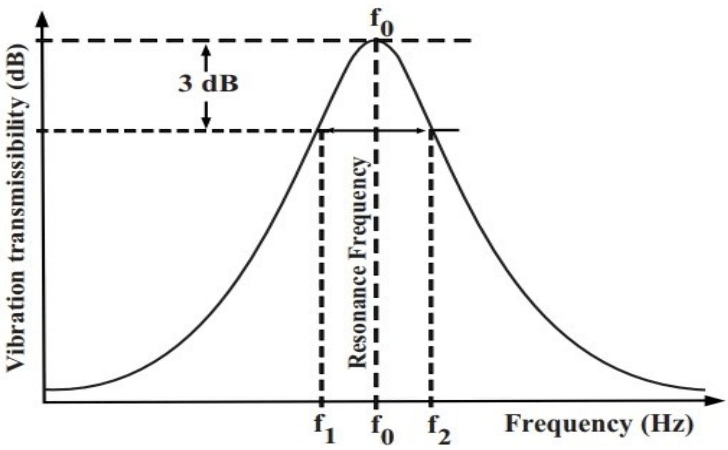

Figure 2 Frequency spectrum for half power band width method.

The output of the vibration exciter is used to plot transmissibility versus the frequency graph of various elastomeric bearings. Transmissibility analysis is done only on the *Z*-axis as the resonance frequencies in the *X* and *Y* axes are less than that of the *Z*-axis. If the transmissibility characteristics are acceptable along the *Z*-axis, it can also be acceptable in the X and Y directions. Thus vibration transmissibility is evaluated for all frequencies ranging from 10Hz to 4000 Hz for a sine wave harmonic vibration in the *Z*-axis direction. For generating the transmissibility curve, vibration transmissibility at each frequency is calculated in dB as in Eq. (2).

$$\text{Transmissibility} = 20\times\log\left(\frac{\text{Acceleration on top plate}}{\text{Acceleration on bottom plate}}\right) \tag{2}$$

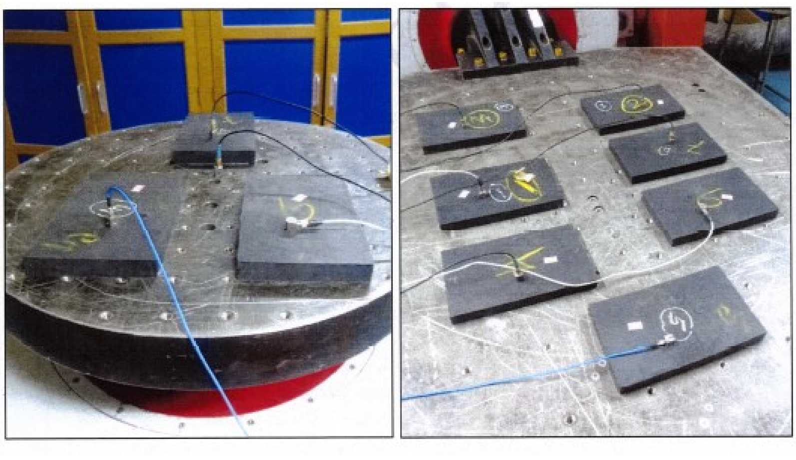

Figure 3 Photograph of elastomeric bearings in Z axis & X axis, respectively.

The vibration transmissibility of elastomeric bearings with different materials was measured at Vibration Test Facility in the Naval Physical and Oceanographic Laboratory, Kochi, for l0 to 4000 Hz frequency in the X, Y, & Z axes. The rubber pad foundation, accelerometer base, and shaker head were cleaned and the rubber pad was mounted on the shaker head along Z-axis. The control accelerometer was pasted on an expander and the setup was excited by a random vibration source with a power spectral density (PSD) of 2.52×10^{-4} g^2/Hz (equivalent amplitude l g_{RMS}) for all three axes. The output of the rubber pad top and control accelerometer were measured and vibration transmissibility was calculated.

Numerical analysis

The finite element analysis of the elastomeric bearing with different damping materials was conducted *using* ANSYS and calculated its loss factor. The geometry of the elastomers is shown in **Figure 4**, which is $125\times200\times20$ mm^3. The geometric and material modelling of the elastomeric bearings is done. In addition, experimentally obtained stress-strain data of the elastomers from the Universal Testing Machine are used to model the non-linear behaviour of the elastomeric bearings. The stress-strain data of each elastomer were found from the tensile test. Then the density and stress-strain data of each elastomer were imported into Ansys for the structural analysis. The stress-strain data was imported into the multilinear isotropic hardening in the plasticity tool. The accuracy of results obtained in finite element analysis depends on the quality of mesh used for analysis. The numerical analysis was carried out with 374, 500 and 976 elements. However, the area of hysteresis loop was similar in all cases. Hence meshing using 374 elements was selected for the study and all the elastomeric bearings are divided into 374 elements with 2286 nodes for numerical analysis.

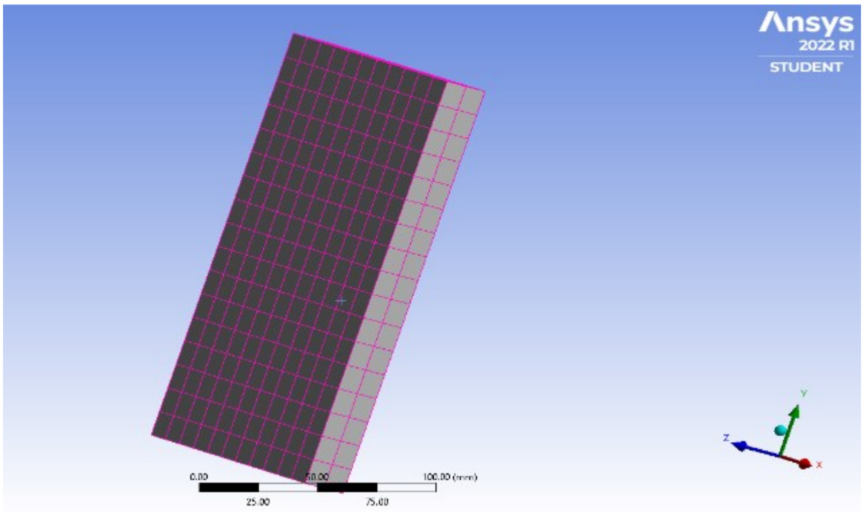

Figure 4 Geometric modelling of the elastomeric bearing.

Stiffness, $K = 4\,\pi^2 f^2 M$ (3)

Maximum strain energy, $U = \pi\, K\, X^2$ (4)

Loss factor, $\eta = \Delta U / U$ (5)

The hysteresis curve obtained from the vibration isolator subjected to a cyclic displacement is set as a condition for finite element analysis. The bottom surface of the elastomeric bearings is fixed. A cyclic displacement with a maximum displacement of 2 mm was applied on the top plate of the isolator in the Z direction for 4 s. Modal analysis is done with the same data as static structural analysis and the model frequency of each elastomeric bearing is evaluated. This modal frequency is used for the theoretical calculation of the loss factor of elastomers. The area under the hysteresis loop was calculated by the vector method. Then the modal analysis of the isolator was carried out from which natural frequencies were found. Then stiffness (k) is calculated using Eq. (3), where M *and* f are the mass of the isolator and the natural frequency from the modal analysis. Then, the maximum strain energy or work done by the harmonic force/ cycle (U) is calculated using Eq. (4), where X is the maximum deformation in the cycle. Eq. (5) is used to determine the loss factor (η), where ΔU is the area under the hysteresis loop.

Results and discussion

The graph shown in **Figure 5** is the output of the vibration exciter machine which shows the vibration transmissibility (dB) of various elastomeric bearings at different frequencies ranging from 10 to 4000 Hz. **Figure 5** shows that Neoprene (CR) is having maximum transmissibility at the resonance frequency (1500 Hz) so it will have the least damping among the Natural Rubber (NR), Styrene Butadiene Rubber (SBR) and Neoprene (CR). However, Styrene Butadiene Rubber (SBR) is having greater loss factor and hence NR and SBR combinations were made by changing the rubber ratios and studied its damping effects.

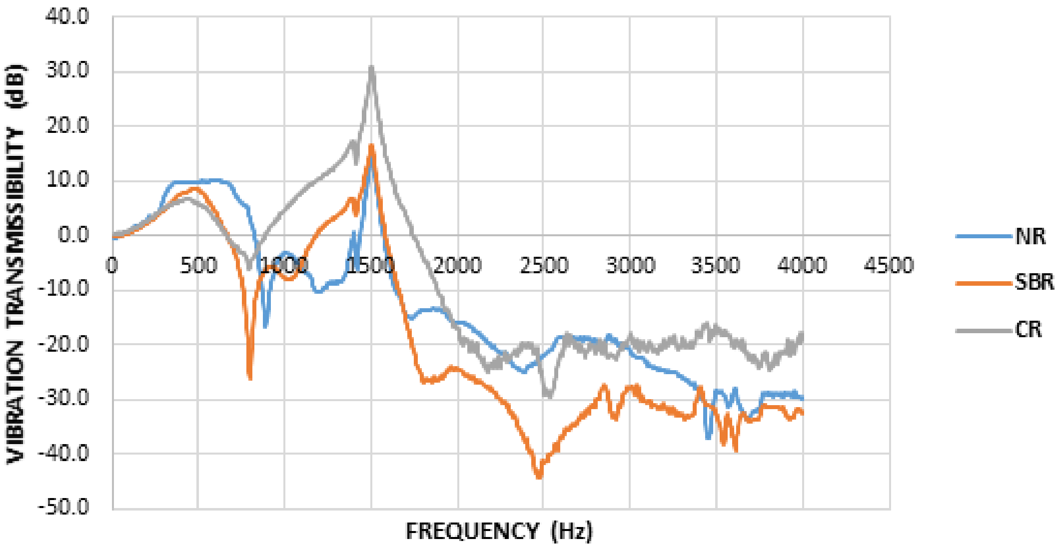

Figure 5 Vibration transmissibility vs frequency graph of NR, SBR and CR.

Figure 6 is a comparative study of vibration transmissibility of NR and SBR combinations. The results show damping property of natural rubber increases with the increase in the percentage of SBR. The NR-SBR (25:75) is having maximum loss factor and thus it can be considered a good vibration isolator among all the combinations of NR-SBR. **Figure 7** is a comparative study of vibration transmissibility of NR-SBR and NR-PBR. This comparison is taken because PBR and SBR belong to butadiene rubbers. When blended with natural rubber, NR-PBR (50:50) gives a maximum loss factor compared to NR-PBR (50:50).

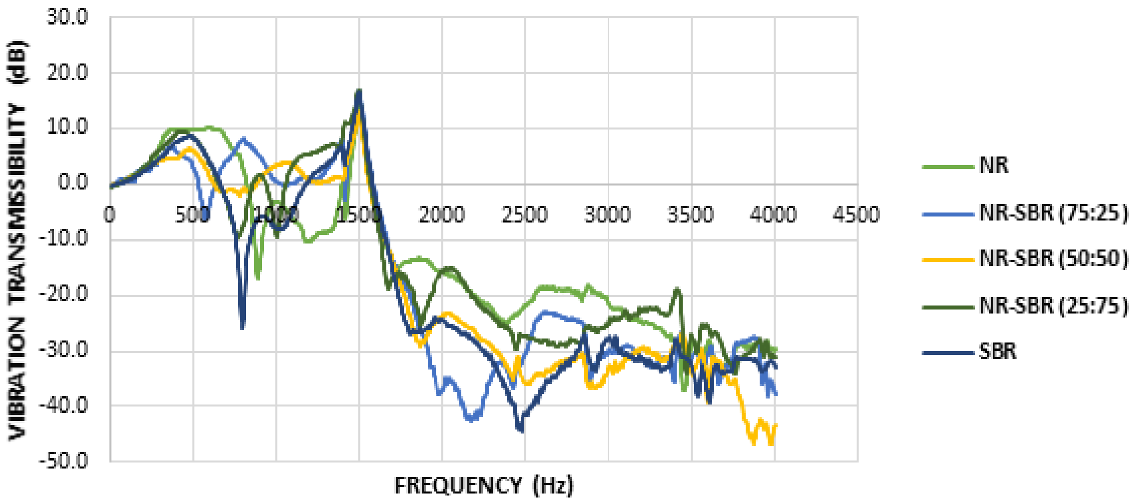

Figure 6 Vibration transmissibility vs frequency graph of NR-SBR combinations.

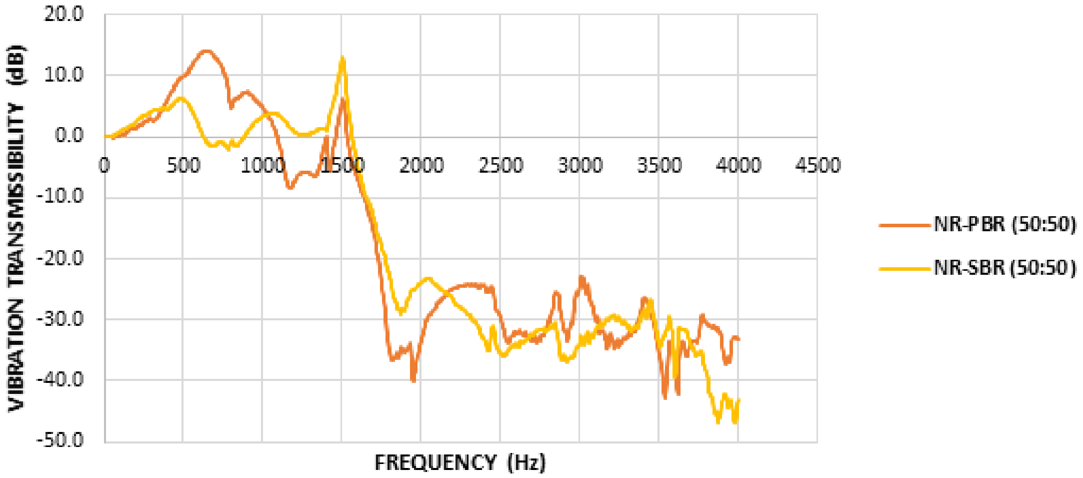

Figure 7 Vibration transmissibility vs frequency graph of NR blended with PBR and SBR.

From experimental analysis, NR-PBR (50:50) is having maximum loss factor of 2.68 % as shown in **Table 1**. It was also found that the damping property of natural rubber goes increasing with an increase in the ratio of SBR. Moreover, NR-SBR (25:75) is showing good damping with a loss factor of 2.60 %.

Table 1 Loss factor by experimental method.

Sl. No.	Material	F_0 (Hz)	Transmissibility (dB)	Transmissibility -3 dB (dB)	F_1 (Hz)	F_2 (Hz)	Loss Factor $(F_2 - F_1)/F_0$ (%)
1	NR	1500	14.8	11.8	1486	1520	2.26
2	SBR	1500	16.5	13.5	1482	1520	2.53
3	CR	1500	30.7	27.7	1485	1520	2.33
4	NR-SBR (75:25)	1500	16.9	13.9	1483	1520	2.46
5	NR-SBR (50:50)	1500	13	10	1480	1518	2.53
6	NR-SBR (25:75)	1500	16.9	13.9	1478	1517	2.60
7	NR-PBR (50:50)	1500	6.3	3.3	1418	1512	2.68

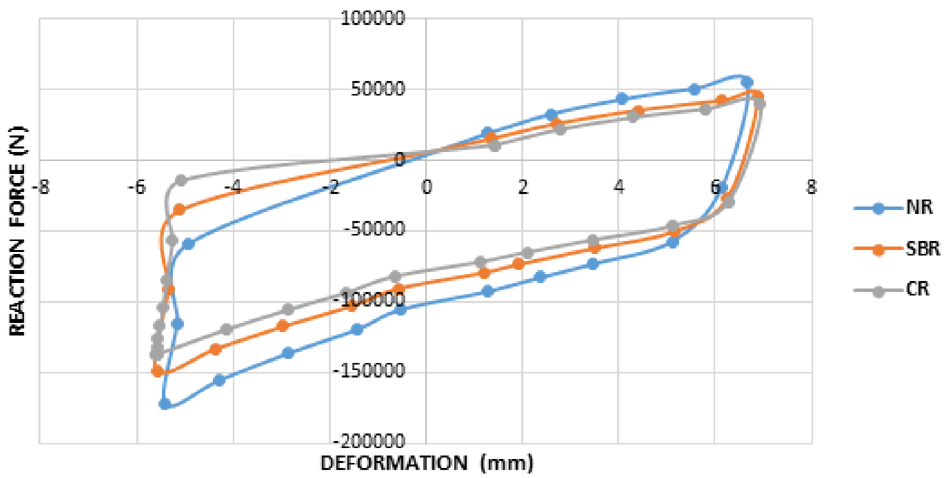

Figure 8 Hysteresis curve of NR, SBR and CR.

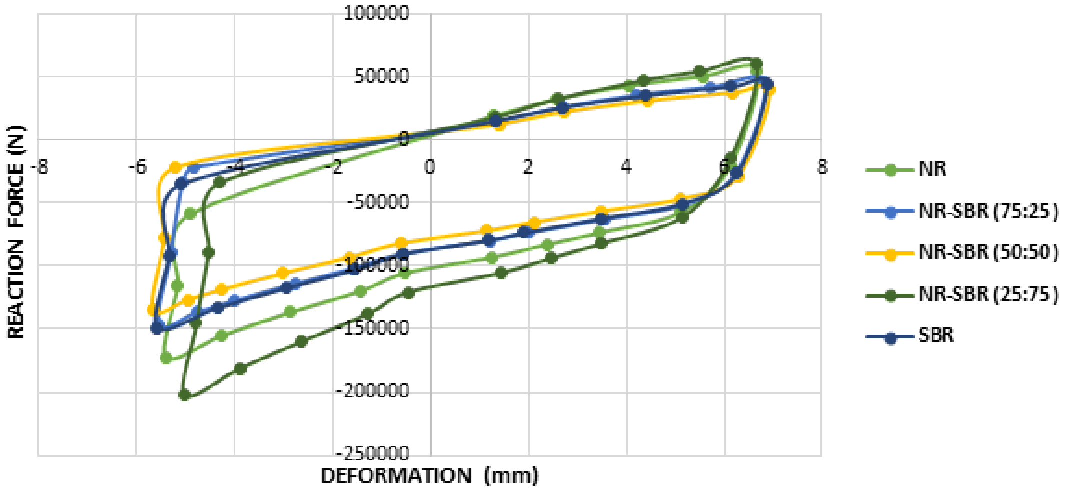

Figure 9 Hysteresis curve of NR-SBR.

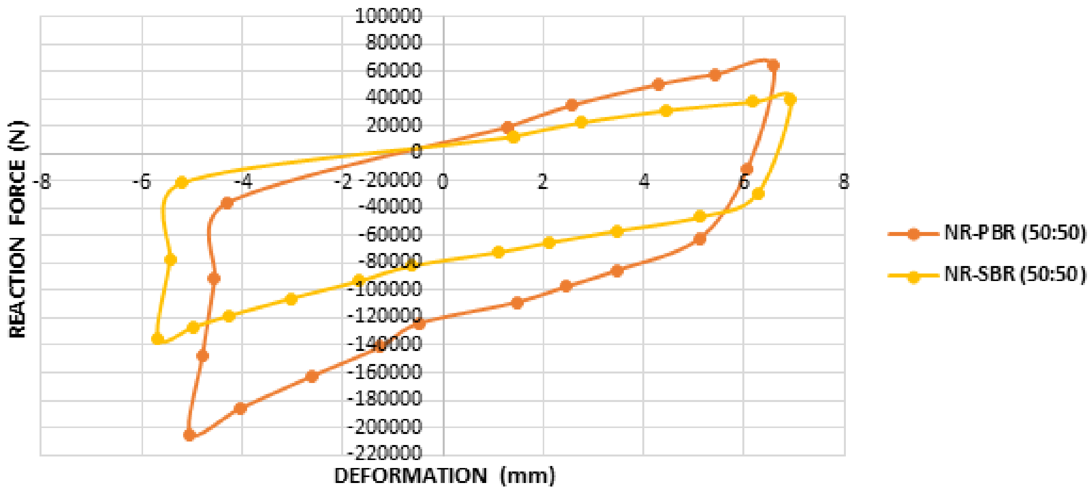

Figure 10 Hysteresis curve of NR blended with PBR and SBR.

As shown in **Figure 8** the hysteresis curve of elastomeric bearings was plotted using the results from the static analysis. The area of the hysteresis curve of the natural rubber was found to be greater than neoprene and styrene-butadiene rubber. However, it has the lowest value of maximum deformation. The area of natural rubber was 1202927.65 Nmm and the maximum deformation was 6.668 mm. Similarly, the hysteresis loop of NR-SBR combinations was plotted in **Figure 9**. The hysteresis curve of NR blended with PBR and SBR has shown in **Figure 10**. NR-SBR (50:50) was having the greatest value of maximum deformation from the above combinations. However, NR-PBR (50:50) was having maximum area from the above hysteresis loops hence it will have the maximum energy dissipation, *i.e.*, it has the maximum loss factor among the above combinations.

Table 2 shows the modal frequency, maximum deformation and loss factor from numerical analysis. The area of the hysteresis loop was calculated using the vector method and got the maximum deformation from the hysteresis loop. The modal frequencies of each elastomeric bearing were calculated using finite element analysis. The NR-PBR (50:50) is having the least value of maximum deformation and the highest area from the hysteresis curves. Hence it is the best elastomeric compound for damping as per the numerical analysis. Moreover, NR-PBR (50:50) is having a maximum loss factor of 2.76 % followed by NR-SBR (50:50) with a loss factor of 2.75.

Table 3 shows the comparison between numerically and experimentally calculated loss factors of different materials. As the values of loss factors obtained from both methods are practically the same and hence the methodology for the generation of the hysteresis curve and loss factor is validated.

Table 2 Modal frequency, maximum deformation, mass of elastomers and loss factor from numerical analysis.

Sl. No.	Material	Area of hysteresis loop, ΔU (Nmm)	Modal frequency, f (Hz)	Max deformation, X (mm)	Mass, M (g)	Stiffness, K (N/mm)	Max Strain Energy, U (Nmm)	Loss factor (η) (%)
1	NR	1202927.65	4093.9	6.66	565	373837.31	52218416.76	2.30
2	SBR	1097948.08	3776.4	6.86	540	304031.56	45027324.84	2.43
3	CR	1050511.35	3689.7	6.93	575	309036.44	46679612.39	2.25
4	NR-SBR (75:25)	1130108.45	3815.7	6.82	545	313259.81	45868481.36	2.46
5	NR-SBR (50:50)	1045793.87	3553.3	6.93	550	274148.69	41433747.64	2.52
6	NR-SBR (25:75)	1359185.90	4027.0	6.65	555	355316.99	49393560.47	2.75
7	NR-PBR (50:50)	1376910.50	4013.6	6.58	580	368855.19	49715107.06	2.76

Table 3 Comparison between the numerically and experimentally calculated loss factors.

Sl. No.	Material	Numerically calculated Loss factor (Hysteresis method) (%)	Experimentally calculated Loss factor (3 dB method) (%)	Percentage Error in numerical analysis (%)
1	NR	2.30	2.26	1.76
2	SBR	2.43	2.53	3.95
3	CR	2.25	2.33	3.43
4	NR-SBR (75:25)	2.46	2.46	0
5	NR-SBR (50:50)	2.52	2.53	0.39
6	NR-SBR (25:75)	2.75	2.60	5.76
7	NR-PBR (50:50)	2.76	2.68	2.98

Conclusions

A passive vibration isolator uses the inherent properties of the isolation device to mitigate vibrations and therefore requires no external power source to store or dissipate energy. The elastomeric bearing with Natural Rubber (NR), Styrene-Butadiene Rubber (SBR), Poly Butadiene Rubber (PBR), Neoprene (CR) and their combinations are fabricated and the loss factors of each material were determined numerically and experimentally. The values of the loss factor obtained from both methods are agreeable. In the first phase Natural Rubber, Styrene Butadiene Rubber and Neoprene were compared based on their loss factor. Styrene-Butadiene Rubber was found to have a maximum loss factor and hence Natural Rubber and Styrene-Butadiene Rubber combinations were fabricated by changing their rubber ratios. The second phase result shows that the damping property of Natural Rubber goes increasing with an increase in the ratio of Styrene-Butadiene Rubber. The NR-SBR (25:75) showed a maximum loss factor of 2.60 %. Therefore, in the third phase, a comparative study was made between equal ratios of Natural Rubber blended with Styrene-Butadiene Rubber and Poly Butadiene Rubber. The results showed that both Butadiene rubbers were having good damping. However, compared to NR-SBR, NR-PBR (50:50) has the greater loss factor. Thus, NR-PBR (50:50) and NR-SBR (25:75) have the maximum loss factors. Hence can be used as dampers for high-frequency applications. Moreover, the results indicate that blending Natural rubber (NR) with Styrene butadiene rubber (SBR) or Poly butadiene rubber (PBR) increases the damping properties of the elastomers. A loss factor of 2.68 % is achieved from the fabricated NR-PBR (50:50) bearing.

References

[1] S Krishnamoorthi, S Nagendharan and RS Praveen. Investigation of vibration behavior of fluorocarbon mounts. *Int. Res. Eng. Tech.* 2018; **5**, 3051-4.

[2] H Wan, Y Li and L Zheng. Vibration and damping analysis of a multilayered composite plate with a viscoelastic mid layer. *Shock Vib*. 2016; **2016**, 6354915.

[3] RA Ibrahim. Recent advances in nonlinear passive vibration isolators. *J. Sound Vib.* 2008; **314**, 371-452.

[4] VS Chavan, R Askhedkar and SB Sanap. Analysis of anti-vibration mounts for vibration isolation in diesel engine generator set. *Int. J. Eng. Res. Appl.* 2013; **3**, 1423-8.

[5] A Valeev, A Zotov and S Kharisov. Designing of compact low frequency vibration isolator with quasi-zero-stiffness. *J. Low Freq. Noise Vib. Active Contr*. 2015; **34**, 459-73.

[6] PS Bharat, BB Shivprakash, GT Sandeep and M Samata. Design and analysis of antivibration mount for G+3 elevator. *Int. J. Curr. Eng. Tech.* 2014; **7**, 103-8.

[7] SS Devi, M Niveshim, R Subesh and M Rohan. Experimental behaviour of elastomeric bearing on bridge structures. *Int. J. Recent Tech. Eng*. 2019; **8**, 7856-9.

[8] M Ahmadipour and MS Alam. Sensitivity analysis on mechanical characteristics of lead-core steel-reinforced elastomeric bearings under cyclic loading. *Eng. Struct.* 2017; **140**, 39-50.

[9] A Mathai and MS Manasa. Performance of lead rubber bearing as a base isolator. *Int. J. Sci. Tech. Eng.* 2017; **3**, 33-6.

[10] A Das, A Dutta and SK Deb. Modelling of fibre-reinforced elastomeric base isolators. *In*: Proceedings of the 15th World Conference on Earthquake Engineering, Lisbon, Portugal. 2012.

[11] BY Moon, GJ Kang, BS Kang and DS Cho. Design of elastomeric bearing system and analysis of its mechanical properties. *J. Mech. Sci. Tech.* 2004; **18**, 20-9.

[12] A Krishnamoorthy and M Jayavel. Design and analysis of vibration isolation pad of a heavy load machine and to perform the progressive rate frequency analysis. *ARPN J. Eng. Appl. Sci.* 2017; **12**, 4709-16.

[13] SP Barale and SS Gawade. Internal combustion engine vibrations and vibration isolation. *Int. J. Sci. Eng. Res.* 2017; **8**, 243-7.

[14] AR Lavhande and SB Tuljapure. Comparison of transmissibility of non-metallic materials for vibration isolation. *IOSR J. Mech. Civ. Eng.* 2013; **4**, 57-61.

[15] VG Geethamma, R Asaletha, N Kalarikkal and S Thomas. Vibration and sound damping in polymers. *Resonance* 2014; **19**, 821-33.

[16] JH Lee, KJ Lee, HG Park and JH Kim. Possibility of air filled rubber membrane for reducing hull exciting pressure induced by propeller cavitation. *Ocean Eng.* 2015; **103**, 160-70.

[17] M Moshrefi-Torbati, JA Forrester, AI Forrester, AJ Keane, MJ Brennan and SJ Elliott. Novel active and passive anti-vibration mountings. *J. Sound Vib.* 2012; **331**, 1532-41.

[18] X Zhao, J Yang, D Zhao, Y Lu, W Wang, L Zhang and T Nishi. Natural rubber/nitrile butadiene rubber/hindered phenol composites with high-damping properties. *Int. J. Smart Nano Mater*. 2015; **6**, 239-50.

[19] S Emad and TN Hamid. Finite element modelling of horizontal load displacement hysteresis loops in unbonded elastomeric isolators. *Structures* 2021; **34**, 2987-95.

[20] KN Kalfas, AM Stergios and K Katakalos. Numerical study on the response of steel-laminated elastomeric bearings subjected to variable axial loads and development of local tensile stresses. *Eng. Struct.* 2017; **134**, 346-57.

[21] W Wei, P Tan, Y Yuan and H Zhu. Experimental and analytical investigation of the influence of compressive load on rate-dependent high-damping rubber bearings. *Constr. Build. Mater.* 2019; 200, 26-35.